Challenging the traditional model of gear vibration signals

E. Hubert[1], P. Borghesani[2], R.B. Randall[2], M. El-Badaoui[1]
[1]SAFRAN Tech, Rue des Jeunes Bois – Châteaufort, 78772 Magny les Hameaux, France
[2]School of Mechanical and Manufacturing Engineering, UNSW Sydney, NSW 2031, Australia

Abstract

Despite rarely being made explicit, signal models (and assumptions) for gear vibration have been fundamental in the development of both condition monitoring and operational modal analysis techniques. The analysis (for condition monitoring) or the removal (for OMA) of the dominant gear-meshing component is in fact dependent on the assumption on the number, location and patterns of the corresponding spectral harmonics. This paper discusses in detail the common modelling choices and their consequences for condition monitoring and OMA. The traditional gearmesh-carrier/shaft-modulated model is analysed and two main limitations of current models are highlighted: the additive assumption on the two gear modulating functions and the regularity of their effect on different gearmesh harmonics. The paper uses experimental gear signals to prove the validity of the newly introduced assumptions and to assess their practical significance.

1 Introduction

Gearbox condition monitoring has often been based on simple signal models. Empirical signal models are used as a first approximation of the vibration signal to justify and guide the development of diagnostic signal processing techniques. For this purpose, they are preferred to more detailed physical models (e.g. FEM or lumped parameters) due to their generality and ease of implementation. Empirical signal models aim at reproducing the overall properties of vibration signals, retaining the main time and frequency features that are observed in real signals and can be used for condition monitoring. Despite not requiring the fine-tuning of structural and geometric parameters typical of detailed physical models, correct assumptions on the phenomena generating the vibration are fundamental in developing appropriate empirical signal models.
In the case of spur gears, the main source of vibration comes from the time-varying meshing force generated at the contact point between the pinion and driven gear teeth. The most widely accepted gear-signal model is therefore represented as [1]

$$y(t) = h(t) \otimes g(t) \tag{1}$$

where the gear-related component $y(t)$ of a measured vibration signal results from the convolution (symbol $\otimes$) of the system impulse response $h(t)$ with the gear-meshing forcing function $g(t)$. As usual in rotating machines [2], the true nature of this signal has a hybrid time-angle definition. However, for nominally constant speed, the approximation of linearity between time and angular domain is often assumed. In this case, the easiest way to represent the signal in the frequency domain is probably to define (with approximation) the system transfer function $H(f) = \mathcal{F}\{h(t)\}$ in an equivalent shaft-order domain, adopting the approximate relationship $f \approx \Omega f_1$ where f_1 is the average (and almost constant) shaft speed of a reference gear (in this study we will always use the pinion/input shaft) and Ω is the order coordinate of the same shaft. In this case we can rewrite eq. (1) in the order domain as:

$$Y(\Omega) = H(\Omega f_1) \cdot G(\Omega). \tag{2}$$

In the case of perfect and healthy teeth, the contact force $g(t)$ is theoretically expected to show a gearmesh fundamental frequency (i.e. for a pinion with Z_1 teeth $G(\Omega) \neq 0$ only for $\Omega = kZ_1$), but in practice even imperfections in the manufacturing stage result in tooth-to-tooth variations. These variations are expected to be even more accentuated in the case of localised gear faults (e.g. tooth crack) and are modelled as gear-synchronous modulations of the gearmesh harmonics.

The excitation g is usually modelled in time or in the angular domain θ of the reference shaft (in this case shaft 1) as an amplitude/frequency modulated signal, where the carrier is represented by the dominant gearmesh harmonics and the two modulating functions are synchronous with the two shafts. Actual explicit mathematical expressions of AM/FM signal models are rare, and many studies focus on the simpler AM case only. In this paper we will mainly focus on the implications that arise for condition monitoring and OMA in considering an AM/FM model. A full analytical discussion will be provided for AM-only models, including limitations of common assumptions and further issues encountered when dealing with actual signals. However, considerations on FM and AM/FM models will be provided, without the explicit formulation of full AM/FM signal models (due to their cumbersome expression), but keeping in mind all the major and minor spectral components arising from the combination of all modulating functions.

2 Secondary sidebands

The simplest model of the gear force (often implicitly considered in many condition monitoring studies) includes two purely amplitude modulation components:

$$g(\theta) = c(\theta) \cdot \{a(\theta) + b(\theta)\} \tag{3}$$

where:

- $c(\theta)$ is the gearmesh-periodic dominant effect of the tooth-meshing

$$c(\theta) = \sum_h C_h e^{jhZ_1\theta} \tag{4}$$

  with Z_1 representing the number of teeth of the gear on shaft 1,

- $a(\theta)$ and $b(\theta)$ are a shaft-periodic amplitude modulation functions due to irregularities among the teeth of shaft 1 and 2 respectively (and/or geometric/misalignment issues on the same shaft)

$$a(\theta) = \sum_k A_k e^{jk\theta} \quad \text{and} \quad b(\theta) = \sum_k B_k e^{jk\tau\theta} \tag{5}$$

where $\tau = Z_1/Z_2$ is the gear ratio.
Such AM signal is usually represented as:

$$g(\theta) = \sum_h \sum_k C_h A_k e^{j(hZ_1+k)\theta} + \sum_h \sum_k C_h B_k e^{j(hZ_2+k)\tau\theta}. \tag{6}$$

This formulation shows the main feature of AM gear models: the presence of sidebands around the gearmesh harmonics at orders $hZ_1 + k$ (effect of shaft 1) and $hZ_1 + \tau k$ (effect of shaft 2).

Such a simplified model already poses risks for OMA. In fact, the removal of these harmonics is often considered straightforward by means of established synchronous averaging techniques, using encoders installed on both shafts (or at least on a reference shaft). In most cases, shaft-1 and shaft-2 sidebands are thus removed separately by synchronous averaging over the respective periods. Even in a number of highly rigorous approaches, only one or a few combined periods of the two gears are used for these synchronous averaging operations. This "grand-period" is defined as the interval between the meshing of the same tooth pair, and equivalent to Z_2 periods of shaft 1 or Z_1 periods of shaft 2.

However, considering the physical nature of the AM functions $a(\theta)$ and $b(\theta)$, a multiplicative model is much more justified, i.e. there is no reason why carrier and modulations should be treated differently and a three-term multiplication is more appropriate. This results in the modification of eq. (3) into the following:

$$g(\theta) = c(\theta) \cdot a(\theta) \cdot b(\theta) \tag{7}$$

with a consequent proliferation of sidebands:

$$g(\theta) = \sum_{h} \sum_{k} \sum_{\ell} C_h A_k B_\ell e^{j(hZ_1 + k + \tau\ell)\theta}. \tag{8}$$

Under this modelling assumption – and actually also for model (3) –, the fundamental period of the signal is the "grand-period". However, differently from model (3) the signal shows a vast number of secondary sidebands $hZ_1 + k + \tau\ell$, with $k, \ell \neq 0$ (in addition to the $\ell = 0$ and $k = 0$ primary sidebands present also in the previous model). These secondary sidebands are expected to have (in the spectrum of the excitation) a lower amplitude (as the zero-frequency component of the modulation signals must be dominant to ensure positive-only modulating functions), but they could still significantly compromise OMA attempts based on the assumption that noise dominates the spectrum of the vibration signal, once the primary sidebands are removed.

An experimental test to verify the extent of this effect has been carried out on the UNSW spur-gear test-rig. The test-rig is composed of a speed-reducing spur gear pair ($Z_1 = 27$ and $Z_2 = 44$) powered by an electric drive and connected to a magnetic particle brake. The set of gears (module 2 with 5 mm face width) are built in mild steel, and surface hardened. A gear crack was simulated by means of an artificial slot on the pinion starting at the base of the tooth and reaching the centreline with an angle of 45°. The test rig was operated with constant speed and load (10 Hz /10 Nm on the input shaft) and a vibration signal was measured by means of a B&K4396 accelerometer, installed on the top of the casing in proximity of the DE input-shaft bearing. The signal was sampled at a rate of 100 kSamples/s for a duration of 101 s, sufficient to ensure the observation of 22 "grand-periods". In addition, a phase-reference signal was obtained synchronously to the vibration signal, thanks to an encoder with 1000 pulses/rev installed on the NDE of the pinion shaft.

The vibration signal was order-tracked ensuring that an integer number of samples N_{GM} was taken within a gearmesh period, thus also ensuring integer numbers of samples $Z_1 N_{GM}$ in a revolution of shaft 1 and $Z_2 N_{GM}$ in a revolution of shaft 2. Residuals were obtained following two synchronous averaging (SA) procedures: the first was the traditional approach which removed all harmonics of shaft 1 and shaft 2 (primary sidebands of the gearmesh harmonics), whereas the second used the entire grand-period as reference for the synchronous averaging, thus removing all primary and secondary sidebands.

The results are shown in Figure 1. The raw order-tracked spectrum clearly shows a significant amount of gearmesh harmonics and sidebands, which are only partly removed by the traditional SA approach. Whereas the low-frequency range (up to 10-15 gearmesh harmonics) seems mostly unaffected by the presence of secondary sidebands, in the range from 15 to 30 gearmesh harmonics the removal of the primary harmonics still leaves a large quantity of discrete components, which are identified as secondary sidebands.

(a)

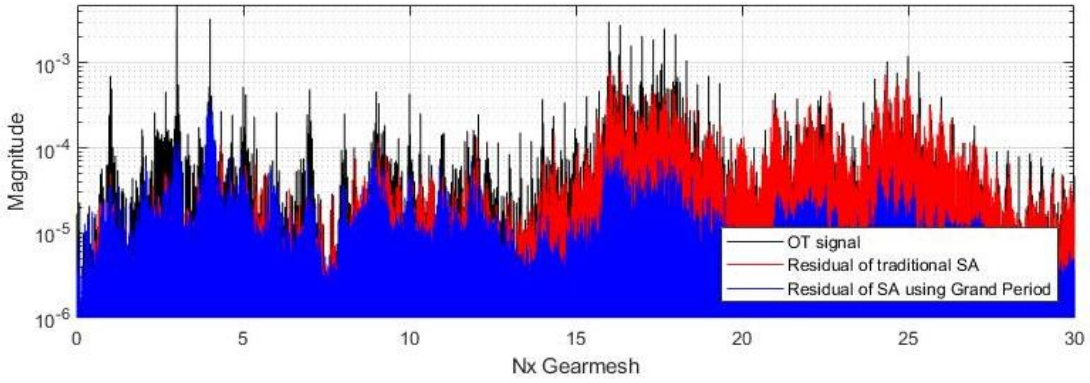

(b)

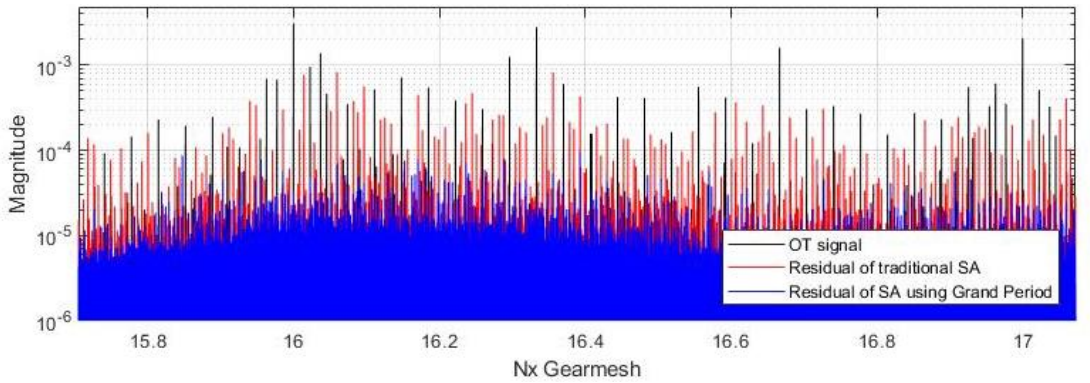

Figure 1. Result of the removal of primary-only (red) and primary + secondary (blue) sidebands from a gear vibration signal (black): (a) frequency range 0-30 gearmesh harmonics, (b) zoom of the most affected area.

Adding frequency modulation to the model, the considerations made so far become even more relevant. Even taking pure frequency modulation, the signal consists of

$$g(\theta) = c\big(\theta + \phi(\theta) + \psi(\theta)\big) \tag{9}$$

where $\phi(\theta)$ and $\psi(\theta)$ are the phase modulations introduced by shaft 1 and 2, respectively:

$$\phi(\theta) = \sum_k \Phi_k e^{jk\theta} \quad \text{and} \quad \psi(\theta) = \sum_k \Psi_k e^{jk\frac{Z_1}{Z_2}\theta} \tag{10}$$

This signal can be expressed as a Fourier Series as:

$$g(\theta) = \sum_h C_h e^{jhZ_1(\theta+\phi(\theta)+\psi(\theta))} = \sum_h C_h e^{jhZ_1\left(\theta+\sum_k \Phi_k e^{k\theta}+\sum_k \Psi_k e^{jk\frac{Z_1}{Z_2}\theta}\right)} \tag{11}$$

The Bessel expansion of such signal (too cumbersome to report in this paper and whose details are of little significance) is composed of a large series of harmonics, at all the multiples of the fundamental frequency obtained from the "grand period". Moreover, whereas the bandwidth of AM sidebands is expected to keep constant for each carrier harmonic, the bandwidth of FM sidebands grows proportionally to the harmonic order of the carrier [3], potentially amplifying this phenomenon at high orders.

A detailed analysis of the motivation (AM, FM or mixed) of the high-frequency location observed for strong secondary side-bands is outside the scope of this paper, but a preliminary sensitivity analysis (varying shaft speed) indicates that the phenomenon has a stable location in the frequency domain (independent of

speed), rather than in the order domain. This suggests that the relevance of the secondary harmonics is linked to a dynamic amplification due to the system transfer function, rather than an FM bandwidth problem.

3 Irregularity of the sideband patterns

According to the AM model of eq. (3), each sideband-pattern should repeat identically at each carrier harmonic. This is simply explained by the convolutive nature of the spectrum of an amplitude modulated signal. For instance, simply dividing each set of sidebands $G(hZ_1 + k) = C_h A_k$ by the corresponding carrier harmonic C_h, the following equivalence should be obtained:

$$\frac{G(hZ_1 + k)}{C_h} = \frac{G(h'Z_1 + k)}{C_{h'}} \quad \forall h, h' \in \mathbb{Z} \tag{12}$$

This ideal property is explicitly at the basis of Ref. [4], which proposed a multi-carrier demodulation method, but partially and implicitly adopted by most studies which arbitrarily use the first or second harmonic for demodulation.

This concept is challenged in this section using a vibration signal measured on the same gearbox as discussed in the previous section, albeit with healthy 20 mm face width gears and a transmission ratio of 19/52. The test was operated at 20 Hz with a load of 20 Nm (all measured on the pinion/input shaft). The sampling frequency was set at 100 kHz for a total duration of the acquisition of 10 s.

The order-tracked signal was split into frequency bands corresponding to the neighbourhood of the first 4 gearmesh harmonics and the different sidebands patterns were shifted to overlap with each other. All sideband amplitude coefficients were divided by the corresponding gearmesh harmonics amplitude coefficient, in order to compute an amplitude ratio. The amplitude ratio of those patterns is reported in Figure 2.

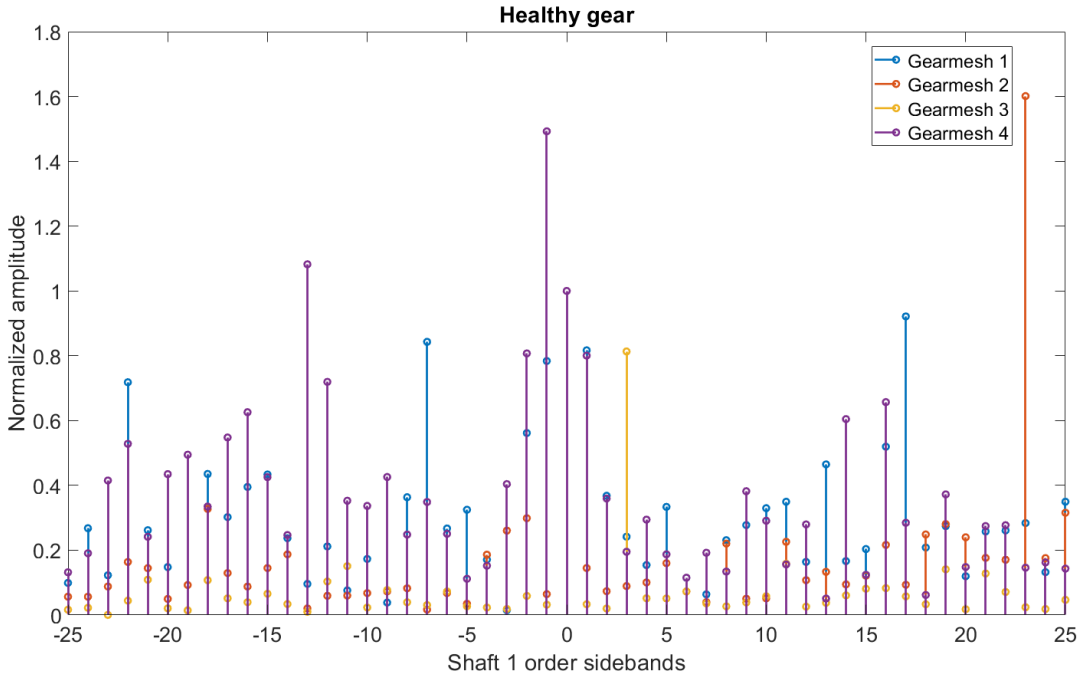

Figure 2. Sideband amplitude patterns of the first 4 gearmesh harmonics. 20 Nm - 20 Hz test.

This result shows how the patterns are massively different even disregarding their phase, which should also coincide after normalisation by the carrier harmonics. Two possible explanations for such behaviour were suggested: amplifications due to the system transfer function, or dominant frequency-modulation effects.

The first option was further investigated trying to remove the transfer function effect by means of cepstral liftering [5], [6]. An exponential lifter was applied, with a cut-off angular quefrency of 0,7 radians,to the original spectrum and the result was used to remove the short-quefrency transfer function effects. The result of the liftering operation and the "normalised" spectrum are shown in Figure 3 (a-b) respectively.

(a)

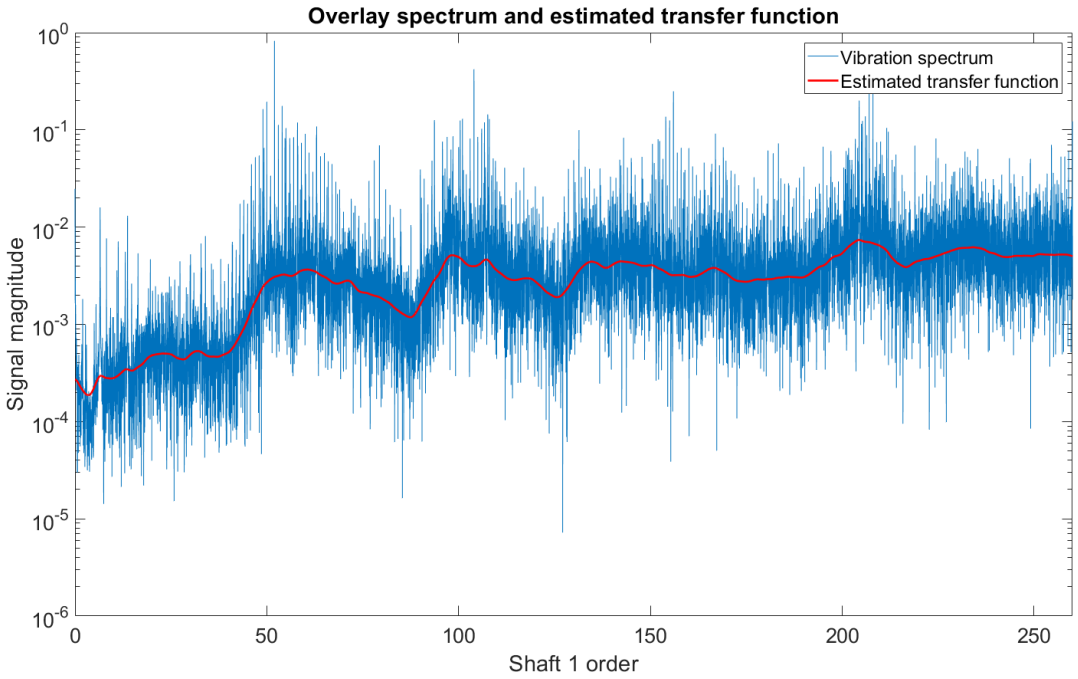

(b)

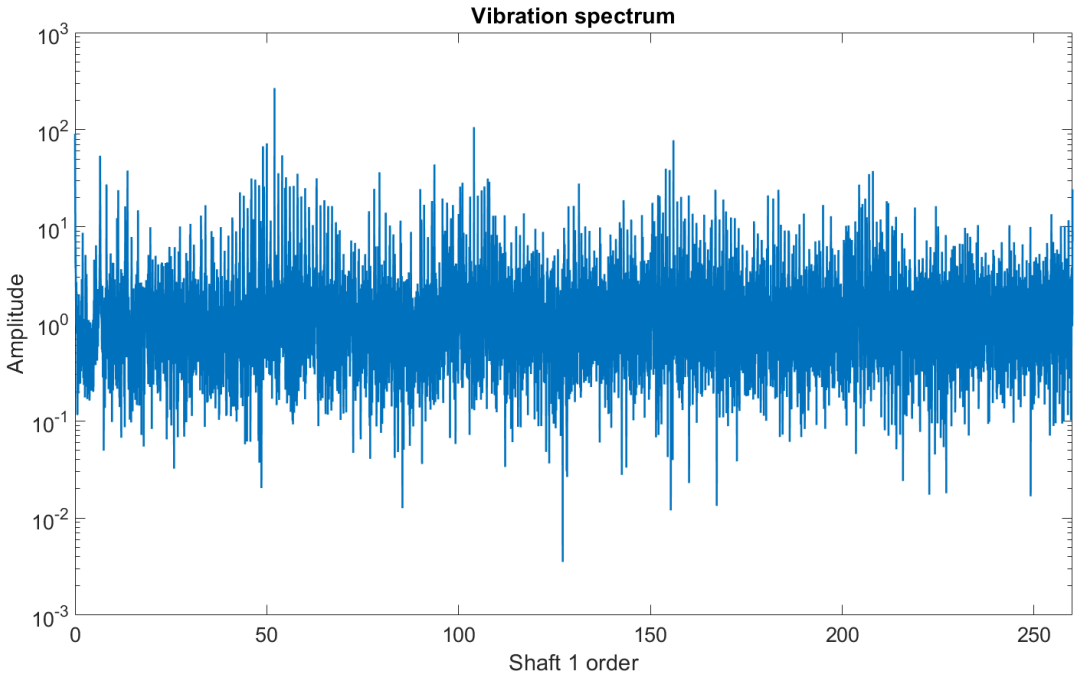

Figure 3. Removal of the TF effect: (a) short-pass liftering operation, (b) normalised spectrum.

Despite the good result in terms of spectral liftering, the problems observed in Figure 2 continue to be as severe in the normalised spectrum harmonics reported in Figure 4.

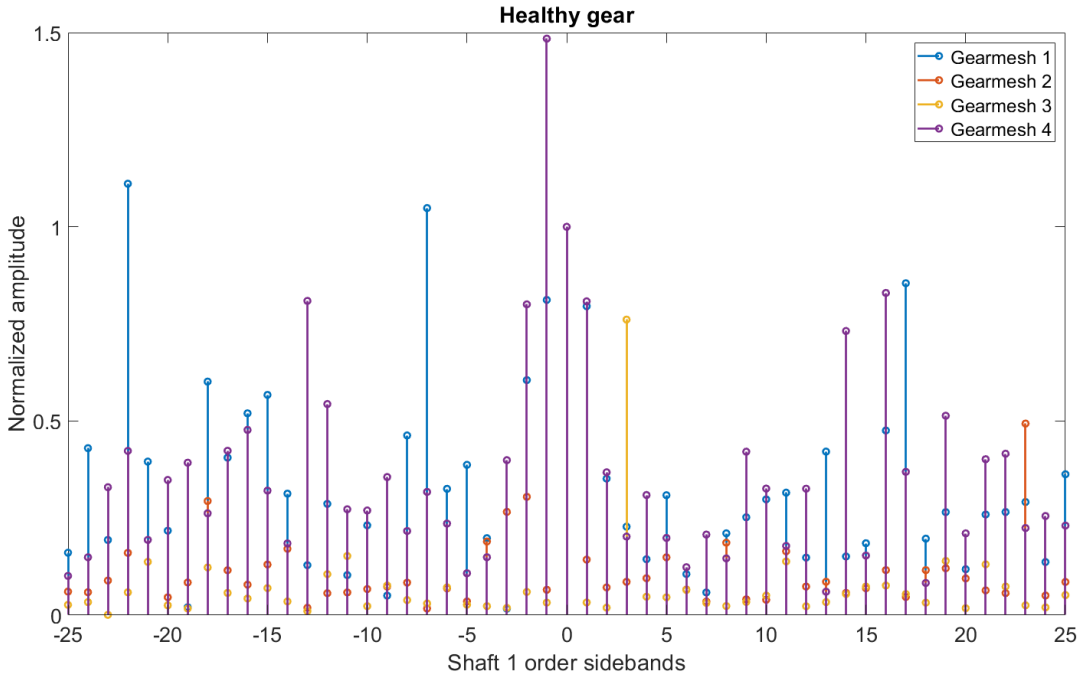

Figure 4. Sideband amplitude patterns of the first 4 gearmesh harmonics after cepstral liftering. ~1.5 Nm - 20 Hz test.

As the shape of the FM patterns of a multi-carrier modulated signal do not seem to match with the ones observed in Figure 2 and Figure 4, the authors are of the opinion that, despite possibly contributing to the difference among the sideband patterns, other phenomena (unmodelled in the current approach) must be influencing the vibration signal. FM multi-carrier modulation in fact usually results in sideband patterns showing a similar "shape", yet with a bandwidth proportional to the carrier harmonic order.

A possible explanation of the differences in the sideband patterns could be found in the different roles played by two different root-cause mechanisms resulting in gear vibration: geometric and static transmission error (each potentially resulting in a separate AM/FM modulated signal, with different carrier and modulation). The first is due to profile irregularities, whereas the second is due to the angular dependence of the gear-meshing compliance under load. An additional test was therefore executed at very low load (~1.5 Nm, just enough to maintain contact between the gear teeth) and speed (2 Hz), where geometric transmission errors were expected to dominate. Since under these operating conditions significant electrical noise was present in the lowest frequency range, in this case harmonics 2-5 were analysed.

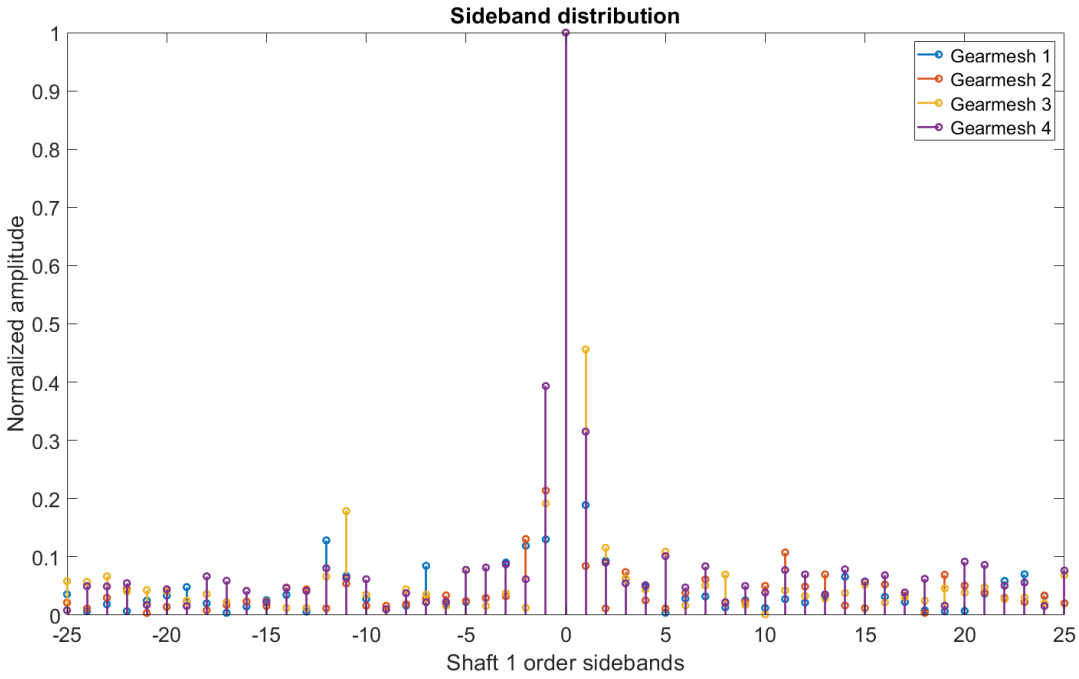

Figure 5. Sideband amplitude patterns of the first 4 gearmesh harmonics. Low load – low speed test.

The patterns shown in Figure 5 are much more consistent, even if discrepancies are still present, thus supporting the idea of a potential two-mechanism root-cause of the observed pattern inconsistency.

In order to investigate more deeply the origin of the pattern inconsistencies observed in the vibration signal, the sideband distribution of the transmission error signal is also studied, in a low-speed and low-load test. As illustrated in Figure 6, the pattern distributions have been plotted for the two cases of a heathy and a faulty gear. The transmission error is computed as the relative difference between the rotation of the input and output shafts. The pattern shown for the sidebands of the healthy gear is almost as consistent as that obtained with the vibration signal, although differences persist in the amplitudes of the sidebands. However, in the case of the faulty gear, the distribution of the sidebands is quite similar for all the sidebands of every gearmesh harmonic.

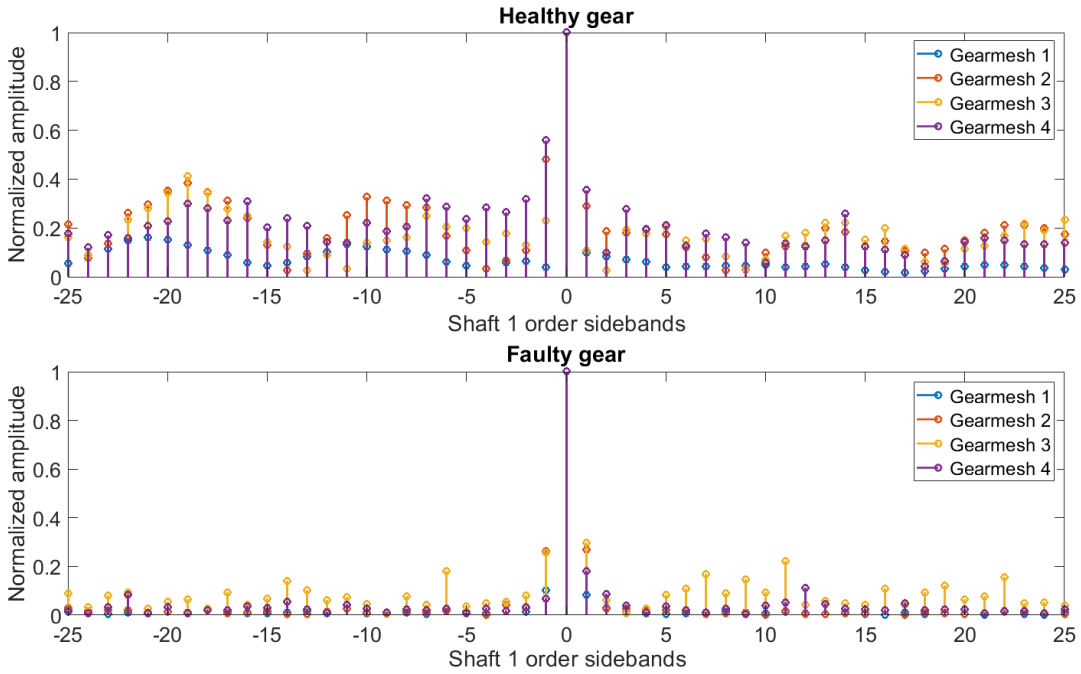

Figure 6: Sideband amplitude patterns of the first 4 gearmesh harmonics of the TE signal. Low load – low speed test.

4 Conclusions

This study has highlighted two major limitations in the current modelling (and assumptions) of gear vibration signals. Neglecting secondary sidebands has been shown to be not always reasonable, and strong discrete components were still observed in the spectrum of a gear signal after removing the primary sidebands by means of traditional synchronous averaging procedures. This problem, which could bias the identification of system transfer functions with OMA approaches, is easily solved if it is possible to observe a sufficient number of "grand-periods". In practice this could be possible for a series of machines operating at reasonably constant speed, but might be impractical for complex transmissions with more than one stage or planetary arrangements (very long grand-period).

Experimental evidence also casts doubts on the validity of AM and even AM/FM models of gear vibration signals, and suggests the possibility of multiple forcing functions (with different spectral distribution) acting simultaneously to create complex modulations. In particular, the geometric vs static transmission error components seem to be potential candidates for future investigations.

Significant investigative efforts are required to clarify these issues and give rise to more reliable models, in turn enabling new and more effective condition monitoring and OMA approaches.

[1] W. D. Mark, “Analysis of the vibratory excitation of gear systems: Basic theory,” *The Journal of the Acoustical Society of America*, 2005.
[2] D. Abboud and J. Antoni, “Order-frequency analysis of machine signals,” *Mechanical Systems and Signal Processing*, 2017.
[3] P. Borghesani, P. Pennacchi, R. B. Randall, and R. Ricci, “Order tracking for discrete-random separation in variable speed conditions,” *Mechanical Systems and Signal Processing*, vol. 30, 2012.
[4] E. Hubert, A. Barrau, and M. E. Badaoui, “New Multi-Carrier Demodulation Method Applied to Gearbox Vibration Analysis,” in *2018 IEEE International Conference on Acoustics, Speech and Signal Processing (ICASSP)*, 2018, pp. 2141–2145.
[5] Y. Gao and R. B. Randall, “Determination of frequency response functions from response measurements - I. Extraction of poles and zeros from response cepstra,” *Mechanical Systems and Signal Processing*, 1996.
[6] R. B. Randall, B. Peeters, J. Antoni, and S. Manzato, “New cepstral methods of signal pre-processing for operational modal analysis,” in *{P}roceedings of the {I}nternational {C}onference on {N}oise and {V}ibration {E}ngineering {ISMA 2012}*, 2012.